Fabrication and characterization of ZnO-based ultra-violet photoconductor and photodetector

SUMIT VYAS
Department of Electronics and Communication Engineering, Thapar University, Patiala-147001, India

In this paper, ZnO thin films were deposited on *p*-type Si substrate and glass substrate using RF sputtering method. Their structural and optical properties were investigated systematically by X-ray diffractometer (XRD), atomic force microscopy (AFM) and ellipsometer respectively. The XRD spectra reveal that ZnO films exhibit wurtzite structure with orientation along (002) plane. The AFM image shows that ZnO thin films exhibit uniform grain with smooth surface. The current-voltage (*I-V*) of Al/ZnO/Al photoconductor and Pd:Au/ZnO/AL photodiode were measured and studied in the dark condition and in the presence of ultra-violet (UV) rays. This work shows the example of fabricating a low-cost and good quality ZnO based photoconductor and photodiode for UV ray detection in the optoelectronic application.

(Received January 25, 2017; accepted November 28, 2017)

Keywords: RF-sputtering, Photo-detector, Photoconductor, ZnO, UV detection

1. Introduction

ZnO is an attractive material for various electronic and optoelectronic devices. The research interest in ZnO for optoelectronic devices has grown enormously because of its large excitonic binding energy of 60 meV at room temperature as compared to 25 meV of GaN, which makes ZnO an efficient light emitter in ultra-violet (UV) and deep blue spectral region [2-3]. Also, the wide band gap of 3.4 eV of ZnO make it sensitive to UV rays compared to the visible and infrared rays. Therefore, one of the main applications of ZnO in optoelectronics field is the detection of UV rays. UV sensors have a wide range of applications. It is used in space application for communication, in the military for missile warning and guiding system. It can be used for monitoring environment as an ozone layer monitor, and for commercial purpose as a fire detector [4-5]. The material to be used for space and military applications should be thermally, mechanically and chemically stable, should have high radiation resistance. ZnO is an ideal material with all these properties along with high gain, and high photoresponse. ZnO is almost transparent in infrared and in the visible region hence ZnO-based UV detector exhibits less dark current and better sensitivity to UV rays as compared to Si-based UV detector [6-12]. Also, high-quality ZnO thin films at room temperature can be deposited by various techniques like radio-frequency (RF) sputtering, sol-gel method [13], thermal oxidation of metallic zinc [14], thermal evaporation of ZnO powder [15], pulsed laser deposition (PLD) [16] and spray pyrolysis [17]. Therefore, due to these various advantages, a high performance with low cost ZnO thin film based devices can be fabricated very easily.

In this paper, ZnO thin films were deposited on p-type Si substrate and glass substrate using RF sputtering method. The photoconduction properties of Al/ZnO/Al in the presence of UV rays and the UV detection property of the Pd:Au/ZnO/Al Schottky diode has been investigated at room temperature and reported systematically.

2. Experimental details

2.1. Cleaning of Wafers

The silicon substrates were cleaned with the RCA-1 solution to remove organic impurities followed by cleaning with the RCA-2 solution to remove any ionic impurities from the substrates. The RCA-1 solution is a mixture of de-ionized (DI) water, NH_4OH, and H_2O_2 in the ratio of 5:1:1 and the RCA-2 solution is a mixture of DI water, HCL, and H_2O_2 in the ratio of 6:1:1. The glass substrate was cleaned ultrasonically in DI water and isopropyl-alcohol. The DI water was obtained from Milli-Q water plant (Millipore, USA).

2.2. Deposition of ZnO Thin Films

The ZnO film was deposited using RF sputtering method. A 50 mm ZnO target was prepared. The ZnO powder (99.99 % pure from Alfa Aesar) was used to prepare the ZnO target. Calculated amount of powder was taken, and few drops of polyvinyl alcohol solution were added. The mixture was made uniform by grinding it for 2 hours using the agate mortar and pestle set. Finally, the ZnO targets was prepared by using hydraulic press set up followed by sintering at 800 ºC in a furnace for 4 hours.

The RCA cleaned substrates and ZnO target were kept in the sputtering chamber, and the chamber was evacuated to a vacuum of 10^{-6} mbar. Highly pure Oxygen (O_2) and Argon (Ar) gas were used for the formation of the plasma in the chamber. The oxygen gas pressure in the chamber was set to 10^{-2} mbar during the deposition. The Ar:O_2 ratio was kept at 10:30 sccm. The pressure in the chamber at the time of deposition, RF power applied, and the thickness of the film were 10^{-3} mbar, 180 Watt and 150 nm to 180 nm respectively. The rate of deposition and thickness was monitored using built-in digital thickness monitor.

2.3. Deposition of Schottky contacts and Ohmic contacts

The Gold:Palladium (Au:Pd in the ratio of 20:80) Schottky contacts have been deposited on the ZnO thin films by using a 2-inch gold palladium target (99.99 % pure) through a brass shadow mask with the circular holes of 1mm in diameter. Sputter Coater was used to deposit the Au:Pd Schottky contact. Similarly, aluminum (Al) contact was formed on ZnO by using a 2 inch Al target (99.99 % pure) through the same shadow mask by RF sputtering method. Fig 1 (a-b) shows the schematic of ZnO based UV photoconductor and photo-diode respectively.

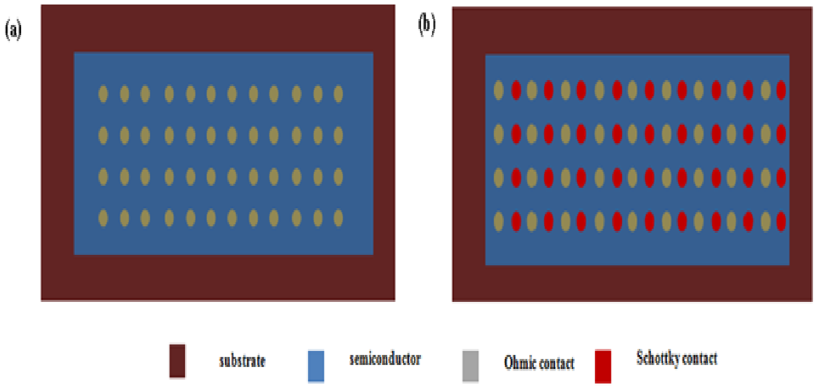

Fig. 1. (a) Schematic of ZnO based photoconductor (b) ZnO based photo-diode.

3. Result and Discussions

3.1. XRD Analysis

Fig. 2 shows the XRD spectra of the ZnO films. X-ray diffractometer (Model: Smart Lab 3kW, Rigaku, Japan with Cu Kα radiation (λ=1.540568 Å)) was used to study the crystal structure of the ZnO thin films. It can be seen from XRD images that, ZnO exhibit hexagonal wurtzite with orientation along (002) plane (confirmed from JCPDS 36-1451: a = 0.3249 nm, c = 0.5206 nm). The peak for (002) plane occurred at 34.43°. The crystallite size, FWHM and interplanar spacing for this plane were 19.22 nm, 0.42°, and 0.26 nm respectively.

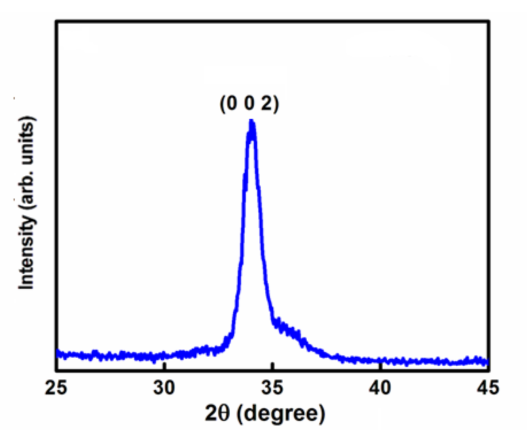

Fig. 2. X-ray diffraction pattern of ZnO thin film deposited on p-type Si <100> substrate by using RF sputtering process

The crystallite size of the deposited films is calculated using Scherrer's equation [18]:

$$D = \frac{0.9\,\lambda}{\beta cos\theta} \tag{1}$$

where D is the crystallites size, λ is the wavelength of X-rays used in XRD, β is the width of peaks at midpoint also known as full-width at half-maximum (FWHM), and 2θ is the angle at which peaks occurred.

3.2. AFM Analysis

Fig. 3(a-b) shows the 2-D and 3-D AFM (Model: Agilent Technologies: 5500) images respectively of the surface of the ZnO thin films deposited on *p*-type Si substrate. It can be observed that ZnO films exhibit smooth surface with a uniform grain distribution of grains. The grain size obtained from the AFM studies were in the range of 120-140 nm. The ZnO films exhibited a certain degree of roughness. The roughness (R_a), the mean roughness (R_q) and total roughness (R_t) of the ZnO thin films were obtained with the help of pico-image software for imaging. The values of roughness was 1.37 nm, the mean roughness was 1.73 nm and the total roughness was 8.69 nm.

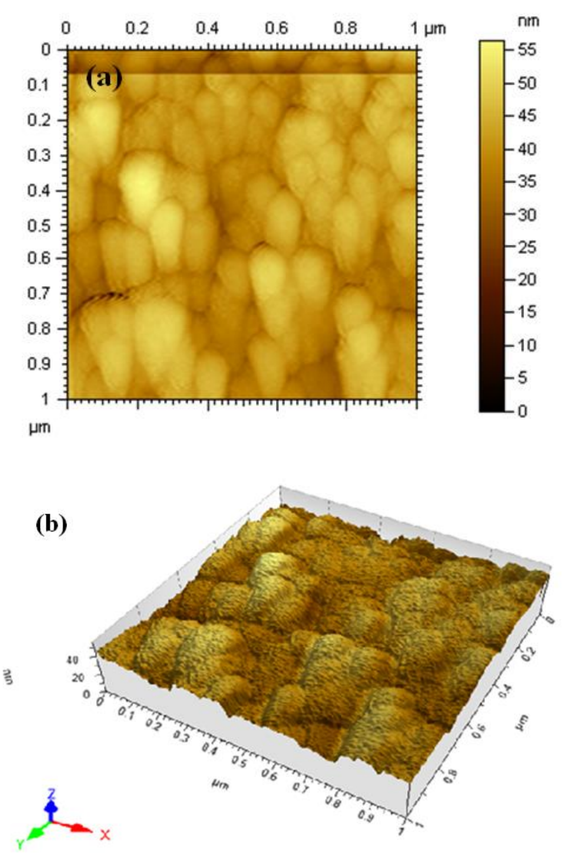

Fig. 3. AFM images of ZnO thin film on p-type Si <100> substrate by RF sputtering process (a) 2-D image (b) 3-D image

3.3. Optical Characterization

The bandgap of ZnO thin films were measured using ellipsometer (Model: J.A Wollam, VB-400). ZnO thin films were deposited on glass substrates and bare glass substrates were used as a reference during measurement. The absorbance spectra with respect to wavelength were obtained with UV-vis measurement. The bandgap of ZnO thin films was extracted from Tauc-plot method, by using the following relation [19]:

$$\alpha h\nu = A \times \left(h\nu - E_g\right)^{1/2} \tag{2}$$

where, α is the absorption coefficient, $h\nu$ is the photon energy, E_g is the optical band gap, A is constant that does not depend on photon energy.

Energy gap E_g was obtained by plotting $(\alpha h\nu)^2$ vs. $h\nu$ and extrapolating the linear portion of $(\alpha h\nu)^2$ vs. $h\nu$ to intersect the $h\nu$ axis as shown in Fig. 4. By using the above method, the bandgap was estimated to be 3.2 eV for ZnO thin films.

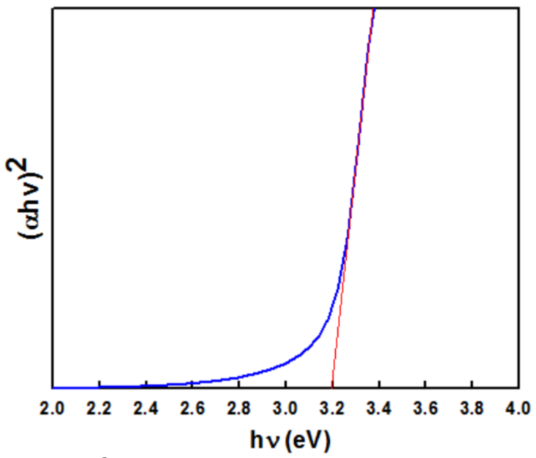

Fig. 4. $(\alpha h\nu)^2$ versus photon energy ($h\nu$) of ZnO thin film on glass substrate by using RF sputtering method.

3.4. UV Photoconductor

Fig. 5 shows the current-voltage (*I-V*) characteristics of Al/ZnO/Al photoconductor measured in the voltage range between -2 V to +2 V under dark and illumination (at the wavelength of 380 nm) with an incident optical power of 0.1 mW at room temperature. It is seen that for a given applied voltage, there is a significant change in current value in the presence of UV radiation at 380 nm. The responsivity (R) of the detector was calculated by using the relation [20]:

$$R = \frac{I_{ph}}{P_{opt}} \tag{3}$$

Here I_{ph} is the current under illumination of UV rays and P_{opt} is the optical power of the incident UV rays. The calculated responsivity at 2 V was 0.135 A/W.

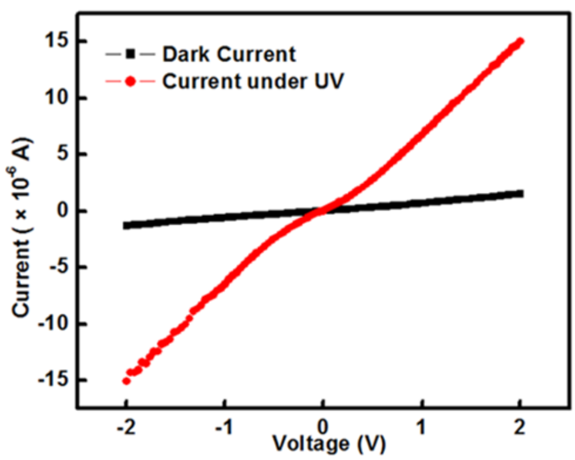

Fig. 5. I-V characteristics of the fabricated Al/ZnO/Al photo-conductor measured in dark and under illumination from -2 V to +2 V

3.5. UV Detection

Fig. 6 shows the *I-V* characteristics of Pd:Au/ZnO/Al measured in the voltage range between -2.5 V to +2.5 V under dark and illumination (at the wavelength of 380 nm) with an incident optical power of 0.1 mW at room temperature. It is seen that for a given applied voltage, there is a significant change in current value in the presence of UV radiation at 380 nm. The responsivity (R) of the detector was calculated by using the relation 3. The calculated responsivity at 2 V was 0.55 A/W.

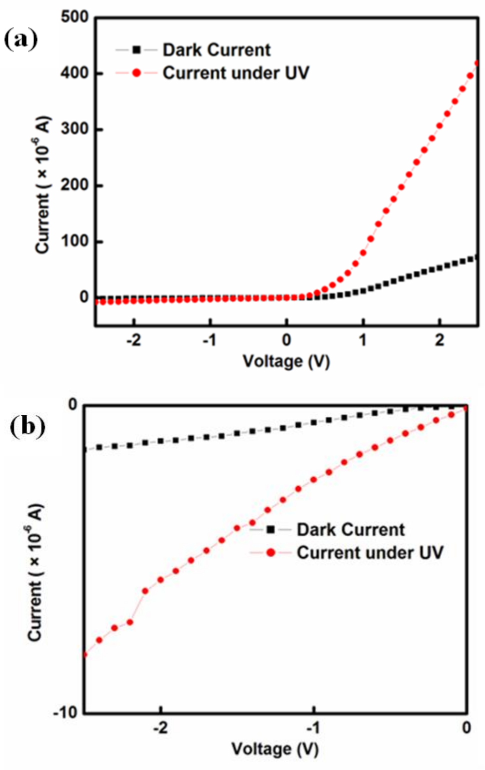

Fig. 6. I-V characteristics of the fabricated Pd:Au/ZnO/Al photodetector measured in dark and under illumination (a) from -2 V to +2 V (b) in reverse bias condition

The barrier height (φ_B) and ideality factor (η) have been calculated for dark current by using thermionic emission theory and the following relations have been used.

$$I_0 = AA^* T^2 e^{-q\varphi/kT} \quad (4)$$

$$I = I_0\left(e^{qV/\eta kT} - 1\right) \quad (5)$$

where η is the ideality factor, k Boltzmann constant, and T is the absolute temperature. *A* is the schottky contact area which is 0.785×10^{-2} cm^2, A^* the effective Richardson constant (theoretically $A^*=32\times10^4$ A cm^{-2} K^{-2}) and φ_B is the barrier height. The reverse saturation current, the ideality factor and barrier height were extracted from the measured *I-V* characteristics and was found to be 20.42 nA, 4.25 and 9.67 eV respectively. The value of the ideality factor is greater than unity. High values of ideality factor can be attributed to the presence of the interfacial thin native oxide and interface defects layer at Au and ZnO interface [21].

4. Conclusion

ZnO thin films were grown by RF-sputtering method and their structural and optical properties were investigated by XRD, AFM and ellipsometer respectively. The XRD spectra reveal that ZnO films exhibit wurtzite structure and the AFM image shows that ZnO thin films exhibit uniform grain with smooth surface. The photoresponse properties of Al/ZnO/Al photoconductor were measured at room temperature. The detector exhibited responsivity of 0.135 A/W at 2 V. The *I-V* characteristics of Pd:Au/ZnO/Al devices under dark and UV illumination were also investigated at room temperature. The Pd:Au/ZnO/Al devices acted as a Schottky diode with rectifying characteristics. The photoresponse properties of Pd:Au/ Schottky contact measured at room temperature. The detector exhibited responsivity of 0.55 A/W at 2 V. This work showed an example of the progress of low-cost and good quality photoconductor for UV detectors in the optoelectronic application and Schottky diode for electronic and optoelectronic applications.

Acknowledgements

The Authors gratefully acknowledge the facilities provided by the Centre for Interdisciplinary Research (CIR), Motilal Nehru National Institute of Technology, Allahabad.

References

[1] Ü. Özgür, Ya. Alivov, C. Liu, A. Teke, M. Reshchikov, S. Doğan, V. Avrutin, S. Cho, H. Morkoc, J. Appl. Phys. **98**, 041301 (2005).
[2] D. Basak, G. Amin, B. Mallik, G. Paul, S. Sen, J. Crystal Growth **256**, 73 (2003).
[3] P. Nayak, J. Jang, C. Lee, Y. Honga, Appl. Phys. Lett. **95**, 193503 (2009).
[4] K. Liu, M. Sakurai, M. Aono, A. Sakurai, M. Aono, Sensors **10**, 8604 (2010).
[5] S. P. Chang, S. J. Chang, Y. Chiou, C. Lu, T. Lin, Y. Lin, C. Kuo, H. Chang, Sens. Actuator A **140**, 60 (2007).
[6] Q. Xu, J. Zhang, K. Ju, X. Yang, X. Hou, J. Cryst. Growth **289**, 44 (2006).
[7] U. Ozgur, D. Hofstetter, and H. Morkoc, Proc. of IEEE **98**, 1255 (2010).
[8] D. Norton, Y. Heo, M. Ivill, K. Ip, S. Pearton, M. Chisholm, T. Steiner, Materials Today **7**, 34 (2004).

[9] S. J. Young, C. C. Yang, L. Lai, J. Electrochem. Soc. **164,** 5 (2017).

[10] S. Liang, H. Sheng, Y. Liu, Z. Huo, Y. Lu, H. Shen, Journal of Crystal Growth **225**, 110 (2001).

[11] S. J. Young, IEEE Sens. J. **11**, 1129 (2011).

[12] L. W. Ji, S. M. Peng, Y. K. Su, S. J. Young, C. Z. Wu, W. B. Cheng, Appl. Phys. Lett. **94,** 203106 (2009).

[13] M. Wang, K. Lee, S. Hahn, E. Kim, S. Kim, J. Chung, E. W. Shin, C. Park, Mater. Lett. **61**, 1118 (2007).

[14] D. Somvanshi, S. Jit, J. Nanoelectron. Optoe. **9**, 1 (2014).

[15] D. Somvanshi, S. Jit, IEEE Trans. Electron Devices **34**, 1238 (2013).

[16] S.-M. Park, T. Ikegami, K. Ebihara, Thin Solid Films **513**, 90 (2006).

[17] D. Afouxenidis, R. Mazzocco, G. Vourlias, P. J. Livesley, A. Krier, W. I. Milne, O. Kolosov, G. Adamopoulos, ACS Appl. Mater. Interfaces **7**, 7334 (2015).

[18] P. Scherrer, Mathematisch-Physikalische Klasse **2**, 98 (1918).

[19] J. Tauc, R. Grigorovich, A. Vancu, Phys. Stat. Sol. **15**, 627 (1966).

[20] S. Young, L. Ji, S. J. Chang, X. L. Duc, J. Electrochem. Soc. **154**, H26 (2007).

[21] M. Asghar, K. Mahmood, M. Faisal, M A Hasan, J. Phys.: Conf. Ser. **439,** 012030 (2013).

*Corresponding author: sumit.vyas@thapar.edu